# Asteroseismological Observations of the Central Star of the Planetary Nebula NGC 1501

Howard E. Bond<sup>1,2</sup>, Steven D. Kawaler<sup>3</sup>, Robin Ciardullo<sup>4</sup>, R. Stover<sup>5</sup>, T. Kuroda<sup>6</sup>, T. Ishida<sup>6</sup>, T. Ono<sup>6</sup>,

S. Tamura<sup>7,8</sup>, H. Malasan<sup>7,9</sup>, A. Yamasaki<sup>7,10</sup>, O. Hashimoto<sup>7,11</sup>, E. Kambe<sup>7,10</sup>, M. Takeuti<sup>7,8</sup>,

T. Kato<sup>12,13</sup>, M. Kato<sup>12,13</sup>, J.-S. Chen<sup>14</sup>, E. M. Leibowitz<sup>15</sup>, M. M. Roth<sup>16,17</sup>, T. Soffner<sup>16</sup>,

and

# W. Mitsch<sup>16</sup>

<sup>1</sup>Space Telescope Science Institute, 3700 San Martin Drive, Baltimore, MD 21218; bond@stsci.edu <sup>2</sup>Guest Observer, Kitt Peak National Observatory, National Optical Astronomy Observatories, operated

by AURA under contract with NSF

<sup>3</sup>Dept. of Physics and Astronomy, Iowa State University, Ames, IA 50011; sdk@iastate.edu

<sup>4</sup>Dept. of Astronomy & Astrophysics, Pennsylvania State University, 525 Davey Lab., University Park, PA 16802; rbc@astro.psu.edu

171 10002, 10C@astro.psu.cuu

<sup>5</sup>UCO/Lick Observatory, University of California, Santa Cruz, CA 95064; richard@ucolick.org

<sup>6</sup>Nishi-Harima Observatory (NHAO), Sayo-cho, Hyogo 679-53, Japan; kuroda@nhao.go.jp

<sup>7</sup>Okayama Astrophysical Observatory, Kamogata-cho, Asakuchi-gun, Okayama 719-02, Japan

<sup>8</sup>Astronomical Institute, Tohoku University, Sendai, Japan 980-77; tamura@astroa.astr.tohoku.ac.jp

<sup>9</sup>current address: Bosscha Observatory, Lembang, Bandung 40391, Indonesia; HAKIM@as.itb.ac.id

<sup>10</sup>Department of Geoscience, National Defense Academy, Yokosuka, Japan 238; yamasaki@cc.nda.ac.jp

<sup>11</sup>Department of Technology, Seikei University, Musashino-shi, Tokyo, Japan 180; hasimoto@aps.seikei.ac.jp

<sup>12</sup>Ouda Observatory, Japan; tkato@kusastro.kyoto-u.ac.jp

<sup>13</sup>Department of Astronomy, Faculty of Science, Kyoto University, Sakyo-ku, Kyoto 606-01, Japan; tkato@kusastro.kyoto-u.ac.jp

<sup>14</sup>Beijing Astronomical Observatory, Chinese Academy of Sciences, Zhongguancun, Beijing 100080, China <sup>15</sup>Wise Observatory and School of Physics & Astronomy, Sackler Faculty of Exact Sciences, Tel Aviv University, Ramat Aviv, Tel Aviv 69978, Israel; elia@wise1.tau.ac.il

<sup>16</sup>Universitäts-Sternwarte München, Scheinerstr. 1, 81679 München, Germany; soffner@usm.unimuenchen.de

<sup>17</sup>current address: Astrophysikalisches Institut Potsdam, An der Sternwarte 16, 14482 Potsdam, Germany;

Received 4 June 1996; accepted 22 August 1996

mmroth@aip.de

# ABSTRACT

We report on a global CCD time-series photometric campaign to decode the pulsations of the nucleus of the planetary nebula NGC 1501. The WC4 central star is an extremely hot, hydrogen-deficient, "O VI"-type object, with some spectroscopic characteristics similar to those of the pre-white-dwarf PG 1159-035 stars. NGC 1501 shows pulsational brightness variations of a few percent with numerous individual periods ranging from 19 to 87 minutes. The pulsation amplitudes and periods are highly variable, suggesting a complex pulsation spectrum that requires a long unbroken time series to resolve. To that end, we obtained CCD photometry of the central star over a two-week period in 1991 November, using a network of observatories around the globe. We obtained nearly continuous coverage over an interval of almost one week in the middle of the run. With this data set, we have identified 10 independent pulsation periods, ranging from 5235 s down to 1154 s. The pulsation modes changed amplitude significantly during the course of the run, indicating either real amplitude variations, or that the modes are not fully resolved over the two-week interval. We find strong evidence that the modes we see in this star are indeed nonradial q-modes. The ratios of the frequencies of the largest-amplitude modes agree closely with those expected for modes that are trapped by a density discontinuity in the outer layers. This conclusion is strengthened by including single-site observations of this star, obtained during previous years, in our analysis. We offer a model for the pulsation spectrum that includes a common period spacing of 22.30 s and a stellar rotation period of 1.17 days; the period spacing allows us to assign a preliminary asteroseismological mass of  $0.55 \pm 0.03 M_{\odot}$ . However, several factors complicate the analysis. Aside from the proximity of the rotational splitting to 1 cycle per day, this frequency splitting corresponds closely to *period* spacings near 20 seconds near the dominant frequencies of the star. Thus, the period spacing and frequency spacings are nearly degenerate.

Subject headings: planetary nebulae: central stars — stars: pulsation — stars: evolution — planetary nebulae: individual (NGC 1501)

# 1. Introduction

A new and powerful tool for probing the depths of white dwarfs is asteroseismology. Stars that are multimode nonradial pulsators can reveal their internal structure through accurate measurements of the periods of their photometric (or radial-velocity) variations. The prototype of the pulsating hot white dwarfs, PG 1159–035 (GW Vir), has yielded a wealth of information about its interior, through analysis of its light curve as obtained by the Whole Earth Telescope (WET); see Nather et al. (1990) for a detailed description of WET. The detailed analysis of WET observations of PG 1159–035 reported by Winget et al. (1991, hereafter "WWET") and Kawaler & Bradley (1994, hereafter KB) illustrates what such stars can teach us; this star shows an unbroken sequence of dozens of pulsation modes that match expectations from stellar evolution and pulsation theory remarkably well. Other GW Vir stars, though they show fewer modes than PG 1159–035, have also been explored in detail through asteroseismology with WET data (i.e., PG 2131+066; Kawaler et al. 1995, PG 1707+427; O'Brien et al. 1997). In addition, PG 0112+200 shows a rich and decodable pulsation spectrum (O'Brien et al. 1996).

As illuminating as the seismological study of the four known pulsating GW Vir-type white dwarfs has been, planetary-nebula nuclei (PNNs) that pulsate have an equally enormous potential as probes of stellar evolution. Nine PNNs are now known to be nonradial pulsators. The first two to be discovered were the nuclei of K 1-16 (Grauer & Bond 1984) and Lo 4 (Bond & Meakes 1990), and six more were discovered in a photometric CCD survey of O VI and PG 1159 PNNs as summarized by Ciardullo & Bond (1996). The total is brought to nine by the discovery of a very faint planetary nebula around the pulsating PG 1159-type star RX J2117.1+3412 by Appleton, Kawaler, & Eitter (1993). (In addition, the PNN-like O VI star Sanduleak 3, although lacking a visible nebula, is a pulsating variable; Bond, Ciardullo, & Meakes 1991.)

Unfortunately, PNNs are more difficult to observe than the pulsating PG 1159 stars for several reasons. One major difficulty is that the pulsation periods of the PNNs range from about 700 s to more than 5000 s, and thus slow transparency variations over a given night make disentangling the true stellar pulsation from variations in the sky transparency difficult. Another problem is that, by definition, PNNs are surrounded by nebulosity. For photoelectric aperture photometry this reduces the measured pulsation amplitude, and causes almost intractable problems due to spurious variations introduced by seeing and small guiding errors. Still another frustration is that in the best-studied pulsating PNN to date, K 1-16, a given pulsation frequency apparently changes significantly from night to night, and changes amplitude irregularly. Despite heroic efforts (for example, see Grauer et al. 1987), the pulsations in K 1-16 have still not been fully resolved. While such instability could result from intrinsic variations in the star, it could also result from beating between modes that are closely spaced in frequency, or from confusion resulting from diurnal aliases or overlapping rotational splittings (see below). This seems to be a property of the entire class; most if not all of the pulsating O VI central stars show complex and variable behavior (Ciardullo & Bond 1996).

Most of the observational problems listed above are solved by global monitoring campaigns with CCD cameras. CCD imaging systems are capable of measuring the relative magnitudes of PNNs on time scales as short as the exposure plus readout time, while the two-dimensional format, which can include simultaneously–observed comparison stars, avoids the problems associated with the nebula and variable sky transparency. In addition, by using a network of CCD-equipped telescopes around the globe, it is possible to obtain nearly continuous data on a specific PNN for a week or more, thus greatly reducing the ambiguities introduced by the daily gaps in single-site data.

In this paper, we report the results of a global observing campaign on the central star of the planetary nebula NGC 1501. NGC 1501<sup>1</sup> was first discovered to be a variable star in 1987 by Bond & Ciardullo (1993). It is classified as a WC4 central star, and shows prominent emission lines of O VI in the stellar spectrum (Smith & Aller 1969; Heap 1982; Kaler & Shaw 1984). Using the HeII Zanstra temperature, Stanghellini et al. (1994) estimate that NGC 1501 has an effective temperature of  $\log T_{\rm eff} = 4.91 \pm 0.03$ ; from its visual magnitude and estimated distance, they obtain  $\log L/L_{\odot} = 3.33 \pm 0.15$ . Comparison of its position in the H-R diagram with evolutionary models (see Figure 9 of Stanghellini et al. 1994) indicates that the mass of NGC 1501 is  $\approx 0.56 M_{\odot}$ . NGC 1501 is very hot, rich in C and O, and hydrogen deficient. It is similar to the PG 1159 spectral class of pre-white-dwarf stars (see, for example, Werner et al. 1991; Werner 1995), although evidently somewhat less evolved. NGC 1501 pulsates on a time scale of about 25 minutes, with an amplitude of up to several percent. In general, therefore, it appears to possess typical properties found in the known pulsating PNNs (Bond et al. 1993; Ciardullo & Bond 1996). Because of the spectroscopic similarities between these stars and the "naked PG 1159 stars" it is presumed that there is a direct evolutionary link, in the sense that the central stars are the precursors of the PG 1159 stars. NGC 1501 is thus an early link in the chain of evolution between stars with active nuclear burning (AGB and post-AGB stars) and stars that are destined simply to cool and fade (white-dwarf stars).

NGC 1501 is probably the best northern PNN candidate for a global monitoring campaign, since it is relatively bright (broadband optical magnitude of about 14), and because its northerly declination  $(+61^{\circ})$ 

<sup>&</sup>lt;sup>1</sup>In this paper we will refer to central stars of planetary nebulae by the names of the nebulae.

makes it observable for nearly 11 hours per night from a single northern-hemisphere observatory during November.

We are entering into a very exciting time in asteroseismology and in the study of PNNs. The NGC 1501 results presented in this paper represent the first detailed analysis of the nonradial pulsations of a PNN. In the next section, we describe the organization of our CCD network for the NGC 1501 campaign, the observing procedures, and the resulting time-series data. We then describe the results of our analysis of the 1991 campaign data, and the pulsation spectrum of NGC 1501. With the aid of our older archival data on NGC 1501, we then construct an initial model of the underlying pulsation spectrum, and obtain the stellar mass and rotation period. We conclude with an attempt to understand this pulsation spectrum in terms of models of PNNs and PG 1159 stars.

## 2. Observations

#### 2.1. CCD Photometry

For 14 days in 1991 November, we monitored the central star of NGC 1501 with 0.8- to 1.0-m telescopes at five sites around the globe: Kitt Peak National Observatory (KPNO) and Lick Observatory in the United States, Okayama Astrophysical Observatory in Japan, Wise Observatory in Israel, and Mt. Wendelstein Observatory in Germany. (Four additional sites also attempted to observe the object during the campaign, but due to weather and technical problems, their contributions could not be used.) At each site, the object was observed throughout the night via a series of short (~ 2 minute) exposures with a CCD detector, and a filter which accepted visual or red light. In all cases, the field of view of the CCD was large enough to include NGC 1501 itself and three nearby comparison stars (shown in Figure 1). A summary of the telescopes and observing setups used in this campaign is presented in Table 1. Table 2 details the active observing time of each observatory. Good weather prevailed at many of the sites, so that between 1991 November 18 and November 28, useful data were obtained for 173 hours out of a possible 216. For example, all nine scheduled nights at KPNO produced usable data (albeit through varying amounts of thin cirrus and haze, which are of little concern for differential CCD photometry). It may be noted that the campaign was centered around full moon, which is not a problem for CCD observations of a star this bright, and made it easier to obtain telescope time.

Our data-reduction techniques are described in detail by Ciardullo & Bond (1996), but are summarized

here. Since each night of observing produced between 200 and 300 CCD images, a frame-compaction algorithm was first used to reduce the data to a manageable size and format. After debiasing and flat-fielding the data, we extracted  $32 \times 32$ -pixel regions surrounding NGC 1501 and its three comparison stars from each individual frame. [Because of the small (0".2/pixel) plate scale of the Okayama observatory data, the frames from this telescope were first binned  $4 \times 4$  before the object extraction took place.] The extracted regions were then moved into a set of "packed" pictures, each containing data from 16 original frames. Although this operation eased the burden of data handling, it in no way affected the subsequent data reductions, since the data from each original frame were always analyzed independently.

Photometric reductions were then accomplished using DAOPHOT algorithms (Stetson 1987) inside IRAF. Each frame's point-spread function (PSF) was first defined using the three pre-selected comparison stars. The relative magnitudes of these stars and that of NGC 1501 were then computed using the DAOPHOT PSF-fitting algorithm with a fitting radius of the order of the image full-width at half-maximum (FWHM). (Because NGC 1501's nebula is of relatively low surface brightness, no special image modeling of the nebula was needed [cf. Ciardullo & Bond 1996]). From these data, NGC 1501's relative intensity was measured by differencing the raw magnitude of NGC 1501 and the flux-weighted mean instrumental magnitudes of the comparison stars.

Because of its favorable declination (+61°), each telescope in our network could observe NGC 1501 for over 10 hours a night. However, during these long runs, the airmass of the object changed substantially. This change, coupled with the color difference between the PNN and our comparison stars (see Table 3 for coordinates and our measured magnitudes and colors), could, in principle, introduce an apparent long-term variation in NGC 1501's brightness, especially in data taken through a broadband filter. We therefore checked for this effect by regressing NGC 1501's computed instrumental magnitude against airmass for each observatory's data, and measuring the slope of the relation. In all cases, the systematic error was  $\lesssim 0.015$  mag per airmass, with a one-sigma uncertainty of about half this value. Since the effect is small, and in any case the time scales of primary interest are significantly shorter than the individual runs, we did not make any correction for differential extinction between NGC 1501 and the comparison stars.

A second correction to NGC 1501's instrumental magnitude comes from the effects of seeing. By restricting our photometry to apertures of the order of the FWHM and treating each frame identically, any error caused by mis-estimating the sky plus nebula surrounding NGC 1501 should have been minimized. However, under conditions of variable seeing, small systematic errors in the relative magnitudes can still exist. To investigate this possibility, we again performed a least squares fit, this time regressing NGC 1501's differential magnitude against the FWHM of the each frame's PSF. Once again, the seeing correction proved to be small, typically less than 0.01 mag per arcsec. As a result, we did not correct for this in the final analysis.

# 2.2. Time-Series Analysis

After obtaining the intensity of NGC 1501 on each individual frame, we computed the "modulation intensity" by subtracting off, and then dividing by, the star's overall mean intensity. After this was done, individual points that were far away from the rest (generally due to cosmic-ray hits on the variable or one of the comparison stars) were edited out, and the observation times were reduced to Barycentric Julian Dynamical Date (BJDD). The data from each site were reduced separately, and then combined into a final light curve. We made no effort to weight the data for the different apertures of the telescopes, CCD sensitivities, or other site-dependent effects.

A subset of the data is shown in Figure 2 in 24-hour strips for seven days at the heart of the run. Figure 2 includes only data from Okayama, KPNO, Wise, and Wendelstein observatories. (Because the Lick data largely overlap those from KPNO, including these data would make the plot more complicated. However, the agreement between observatories is quite good. In the analysis below we do include the Lick data when determining accurate frequencies.) The principal variation of about 1200 to 1500 s is readily visible in this plot. The plot also shows the temporal coverage of our data; the lack of any long vertical stripes without data is an indication that there were no strictly periodic gaps in this segment of the light curve. The window function for this run, obtained by sampling a single-frequency sine wave of fixed amplitude at all of the observed sample times, is shown in Figure 3. The window function has 1 cycle  $day^{-1}$  alias peaks at several percent of the power of the main peak.

We computed the Fourier transform of the reduced data set using a brute-force discrete Fourier transform, and squaring the amplitude of the complex transform to produce the power spectrum. This gives the total modulation power (mp) as a function of frequency. The square root of the modulation power gives the modulation amplitude (ma). In many cases, we find that plots of modulation amplitude (which we call "amplitude spectra") are more useful than power spectra, as the amplitude spectra de-emphasize strong peaks. The representation of pulsation power and amplitude in units of mp and ma is discussed in Winget et al. (1994). The amplitude spectrum is shown in Figure 4 for the entire frequency range of

interest; for comparison, the window function is plotted again, below the strong peak at 866  $\mu$ Hz.

While the amplitude spectrum shows relatively clean peaks, in some cases the (small) alias sidelobes affect the perceived amplitudes and frequencies of lower-amplitude modes. Essentially, the low-amplitude peaks can be shifted away from their true frequencies by power that leaks from the larger-amplitude peaks. Also, the amplitude spectrum does not give a quantitative estimate of the uncertainty in the frequency, amplitude, or phase of a given periodicity. We therefore used a linear least-squares fitting of the time series photometry to determine the precise frequencies, amplitudes, and phases of many peaks simultaneously. Careful use of least squares allows these quantities to be determined accurately for all modes included in the fit (i.e., Kawaler et al. 1995; O'Brien et al. 1996); the least-squares values are unaffected by the sampling pattern if all modes are included in the fit. This procedure also provides a formal estimate of the uncertainty of these quantities.

We used the amplitude spectrum of the entire data set to provide initial guesses for the 11 clearest peaks for use in the initial least-squares fit. The least-squares frequencies match the peaks in the amplitude spectrum within the errors. These frequencies are listed in Table 4. The times of maxima are with respect to  $T_0 = BJDD 2448571.50367$ , which corresponds to a barycentric date of 1991 November 14.0. The only suspicious peak identified in the power spectrum is the peak at 855.5  $\mu$ Hz, which appears to be close to the -1 cycle d<sup>-1</sup> alias of the large peak at 866.3  $\mu$ Hz. Because of its relatively large power, and the difference in frequency between it and the true -1 cycle d<sup>-1</sup> alias, we suspect that it might be a real periodicity in the star. Because of our uncertainty, however, we exclude it in the following analysis.

#### 2.3. Archival Data for NGC 1501

Since only 10 modes were definitively identified in the 1991 global campaign, these data alone are insufficient for the kind of asteroseismological analysis performed on the GW Vir stars. However, other pulsating white dwarfs show modes that appear and disappear on relatively long time scales; when new modes appear, they appear at frequencies expected given the fact that they are g-modes. That is, the new modes usually fit a pattern of equal period spacing and/or rotational frequency splitting. In the case of PNNs, Grauer et al. (1987) and Ciardullo & Bond (1996) show that the modes seen in PNNs can come and go on much shorter time scales than in GW Vir stars. If these modes are indeed normal modes of oscillation, they must occur at the limited set of frequencies fixed by the structure of the star. Therefore, analysis of data taken at earlier seasons could reveal additional frequencies which can be used in the analysis. In the hopes of finding such additional modes, we reexamined time-series photometry of NGC 1501 obtained by Ciardullo & Bond (1996) at KPNO between 1987 and 1990. The individual observing runs are listed in Table 5. Data were obtained using the same CCD system as in the present study, and were reduced following the same procedures as for the 1991 global campaign. Because these were all single-site runs, the power spectra of these additional data are riddled with diurnal aliases. However, in several of the seasons, a few large-amplitude modes can be identified unambiguously. The frequencies, periods, and amplitudes of the dominant modes in those runs are listed in Table 6.

We note that these data sets show abundant evidence for additional periodicities, but the aliasing problem is severe. To disentangle aliases from the true frequencies we followed the prewhitening and synthesis procedures of O'Brien et al. (1996). In some cases we were able to make confident frequency determinations for these runs. In Table 6, the most insecure frequency determinations are indicated with colons (:). A few points are readily apparent. First, the power present in the dominant modes from these runs is much larger than in the 1991 campaign. Moreover, the period with largest amplitude changes from year to year; only in the 1991 data is the 866  $\mu$ Hz mode among the largest. Finally, it is clear that NGC 1501 displayed a number of modes in the recent past that were not present during the 1991 campaign. These additional modes can be used to constrain models of the underlying pulsation spectrum of the star.

# 3. Frequency and Period Patterns in Nonradial g-modes

NGC 1501's pulsation frequencies, if caused by normal nonradial g-modes, should show some systematics. It is these systematics which allow us to place seismological constraints on the global parameters of the star. This section briefly describes some of the systematics of nonradial g-modes that are present in pulsating white dwarfs and that we might expect in the power spectrum of NGC 1501.

# 3.1. Frequency Splitting

One of the observed properties of nonradial oscillations is that equal frequency spacings are often seen when "bands" of power are resolved. For a perfectly spherically symmetric star, the frequencies of all nonradial modes with a given degree  $\ell$  and order n are identical. However, departures from spherical symmetry (which can be caused by rotation, magnetic fields, or some combination thereof) can lift the degeneracy. The most common example is rotation, which splits the degenerate modes into  $2\ell + 1$  components (if all values of the azimuthal index m are present) as follows:

$$\nu_{nlm} = \nu_{nl0} - m \frac{1}{P_{\rm rot}} (1 - C_{nl}), \tag{1}$$

where for white dwarf stars, to within a few percent,

$$C_{nl} = \frac{1}{\ell(\ell+1)} \tag{2}$$

(Brickhill 1975; WWET 1991). Thus, if NGC 1501 rotates, we can expect to see triplets split by one half of the rotation frequency for  $\ell = 1$  modes. We follow the convention that the lower-frequency component of a triplet is identified as the m = +1 component, and the higher-frequency component is labeled as the m = -1 component. Such equally spaced (or nearly equally spaced) triplets are commonly seen in pulsating PG 1159 stars and in the cooler DB and DA white-dwarf pulsators.

## 3.2. Period Spacings

In the limit of high overtones (that is, when the number of radial nodes is much greater than  $\ell$ ) g-modes are approximately equally spaced in period for a given value of  $\ell$  and consecutive values of n, i.e.,

$$\Pi_{nl} = \frac{\Pi_0}{\sqrt{\ell(\ell+1)}} (n+\epsilon), \tag{3}$$

where  $\epsilon$  is a small number. The period spacing ( $\Pi_0$ ) is determined largely by the mass of the star, and is only weakly dependent on the stellar luminosity and surface compositional stratification. KB, and references therein, discuss how the value of this period spacing is used to constrain the mass of GW Vir stars, and how departures from uniform spacing allow the determination of subsurface structure. Since the pattern of equally spaced (in period) multiplets has been seen in several of the GW Vir stars with period spacings of approximately 20-23 seconds, we might expect a similar spacing in the periods of NGC 1501.

The relatively small number of observed modes in NGC 1501, coupled with the long periods and resulting lack of *period* resolution at the frequency resolution set by the run length, makes finding period spacings a difficult task using the 1991 data alone. As we show in the next section, the archival data allow us to identify a possible period spacing.

## 3.3. Strange Frequency Ratios

WWET and KB found that the period spacings seen in PG 1159 itself were not precisely equally spaced. They noted that this could result from mode trapping; that is, a subsurface composition transition region can cause a density discontinuity which acts as a reflecting boundary between the surface and the deep stellar interior. KB identified this layer as the transition zone between the helium-rich surface layer and the carbon/oxygen core. In their analysis, KB computed so-called trapping coefficients, which are related to the frequency ratio of trapped modes. If trapped modes are identified in a star, then the period ratio between the modes can be compared with these coefficient ratios. In fact, the dominant peaks in the amplitude spectrum of the pulsating central star RX J2117.1+3412 show period ratios nearly exactly equal to  $\sqrt{3}/2$  (Vauclair et al. 1996), which is compatible with the coefficients computed by KB. The precision with which the period ratios in RX J2117.1+3412 match  $\sqrt{3}/2$  is remarkable, much better than 1%. This suggests that dominant peaks in RX J2117.1+3412 are indeed trapped modes.

It is immediately apparent that the same ratio exists in NGC 1501. The frequency ratio between the peaks at 866  $\mu$ Hz and 758  $\mu$ Hz is 0.8755, or 1.1% larger than  $\sqrt{3}/2$ . The next two peaks in the sequence would be at about 656  $\mu$ Hz and 569  $\mu$ Hz. We do see a small (but still significant) peak at 661  $\mu$ Hz (at a ratio 0.7% smaller than  $\sqrt{3}/2$ ) and a large peak at 568  $\mu$ Hz (at a ratio 0.8% bigger than  $\sqrt{3}/2$ ). These observed ratios are all much closer to to  $\sqrt{3}/2$  than seen in the theoretical models of KB. Apparently the pulsating central stars NGC 1501 and RX J2117.1+3412 are better calculators of  $\sqrt{3}/2$  than are the computer models!

It is very interesting to see that a large-amplitude mode exists in past data at 656-657  $\mu$ Hz. Figure 5 shows the spectrum of the 1988 data, along with a representative window function. This frequency falls exactly in the  $\sqrt{3}/2$  sequence ratio; the next frequency expected in the sequence below 758  $\mu$ Hz is 656.8  $\mu$ Hz, and the next frequency expected above 567.9  $\mu$ Hz is 655.8  $\mu$ Hz. Thus the archival data strongly support the identification of a series of periodicities with frequencies near the "magic" ratio of  $\sqrt{3}/2$ .

## 4. Decoding the Pulsation Spectrum of NGC 1501

# 4.1. Identification of Rotational Splitting

The 656  $\mu$ Hz periodicity that dominated much of the archival data is not present in the 1991 data, but there is a modest peak at 661.1  $\mu$ Hz. The frequency difference here is about 5.4  $\mu$ Hz. In the 1987 data and the second half of the 1989 data sets, there are clear peaks at 668.0  $\mu$ Hz and 666.3  $\mu$ Hz, respectively. With the 661  $\mu$ Hz peak from the 1991 campaign, these three peaks, seen in different years, may all be components of a uniformly split triplet with  $\delta \nu = 10.2 \ \mu$ Hz. Triplet structures like this are seen in many of the pulsating GW Vir stars; as described in the previous section, it is the expected signature of rotational splitting of  $\ell = 1$  modes. Armed with evidence of a frequency triplet centered near 661  $\mu$ Hz, we used the archival data and campaign data to reveal other evidence for frequency splittings of approximately 10  $\mu$ Hz.

While the 1991 data show an unaliased peak at 567.9  $\mu$ Hz, the strongest peak in the runs kp89-01 and kp89-02 is clearly at 558.0  $\mu$ Hz. This same frequency is present in 1988 data. Figure 6 shows this region of the power spectrum of the 1988 runs. To try to decompose this portion of the spectrum in the presence of 1 cycle/day aliases, we follow the technique of power-spectrum synthesis described in O'Brien et al. (1996). This procedure allows us to find the minimum number of independent frequencies that best reproduce the observed power spectrum. In the top two panels of Figure 6, we show the observed power spectrum as a thick line. In these panels, a thin line shows a synthetic power spectrum created using two sinusoids with amplitudes, phases, and frequencies obtained by least-squares fits to the light curves. The two frequencies used in each synthesis are marked in the figure. The rest of the peaks in the panel arise solely from the window patterns associated with the input frequencies and gaps in the data; no noise was added in this simulation. In the topmost panel of Figure 6, the higher-frequency peak has a frequency close to that seen in the 1991 data ( $\approx 568 \ \mu \text{Hz}$ ). The fitting and synthesis procedure reveals that the two frequencies do not adequately reproduce the observed power spectrum, indicating that either one or both frequencies are incorrect, or that more frequencies are present. However, if we fit the light curve by setting the higher frequency at  $\approx 558 \ \mu\text{Hz}$  (second panel), the entire region is very well matched. Based on this agreement, we are confident that our identification of a 558  $\mu$ Hz periodicity in the 1988 data is correct. Thus there is a pair of peaks separated by about 10  $\mu$ Hz centered at 562  $\mu$ Hz. This is (to within the frequency errors) entirely consistent with the frequency spacings in the 656-666  $\mu$ Hz region.

The archival data support two additional frequency bands with the identified splitting near 530  $\mu$ Hz and 700  $\mu$ Hz. The 1991 data show a peak at 528.3  $\mu$ Hz; the archival data show a peak at 533.5  $\mu$ Hz (in 1988; cf. Figure 6), and at 532.5  $\mu$ Hz (in 1989). Thus, we have evidence for a pulsation mode approximately 5  $\mu$ Hz higher than in 1991. Though there is no evidence of a third peak in this frequency range, the data are consistent with a frequency splitting of modes with the same  $\ell$  and n but consecutive values of m. In 1988, 1989, and 1990 a strong peak was also evident at a frequency of 708  $\mu$ Hz; this peak lies almost exactly 10  $\mu$ Hz above the 698.6  $\mu$ Hz peak seen in 1991.

The mean value of the rotational splitting between the m = +1 and m = -1 modes in NGC 1501 is 9.9  $\mu$ Hz; equations (1) and (2) then imply that NGC 1501 rotates with a period of 1.17 days. If this 9.9  $\mu$ Hz splitting is truly present in NGC 1501, then it would explain why this is such a difficult star to analyze from a single site! The 1 cycle/day alias separation is 11.6  $\mu$ Hz; data from a single site would need to cover at least 11 days to begin to resolve the true power from the alias. Since the modes present in NGC 1501 appear to come and go on this same time scale, identification of the true peaks from a single site is nearly impossible.

## 4.2. Period Spacings

While the number of modes is still a bit small, we can use the measured frequencies in the archival runs, along with the 1991 global campaign, to try to model all of the observed frequencies in terms of modes that are equally spaced in period and rotationally split in frequency with a total splitting of  $\approx 10 \ \mu$ Hz. Unfortunately, to search for period spacings, we need to identify the m = 0 components of the triplets in those cases where all three modes are not present. Complicating matters further, the period spacings are not expected to be precisely uniform, as mode trapping by a subsurface composition transition region could cause small variations in the period spacing with period, as in the pulsating PG 1159 stars (KB).

To compute the period spacings, we begin by determining the periods of the m = 0 modes. The triplet near 656 µHz tells us that the m = 0 central frequency can be estimated when we see two modes separated by 10 µHz. From the frequencies in Tables 4 and 6, we see that m = 0 periods are available for the 563 µHz group, the 661 µHz group, and the 703 µHz group. The differences in these periods are 263 s and 91 s; these should share a common multiple which itself is a multiple of the intrinsic period spacing. The ratio of these is 2.89; that is close enough that we will call it 3; thus the period spacing is either approximately 90 seconds or some integer factor (i.e., 45, 30, 22.5, 18, or 15 seconds).

To reduce this degeneracy, we can appeal to the theoretical calculations of periods and period spacings in PG 1159 stars by KB. Assuming that these are  $\ell = 1$  modes, and that NGC 1501 is a normal planetary-nebula central star, we can eliminate large values for the period spacing. Values above 25 s for the period spacing would imply a mass  $M < 0.5 M_{\odot}$ , well below the minimum mass needed for a single C/O white-dwarf star.

We next consider the mode at 758.5  $\mu$ Hz seen in the 1991 data. With no other nearby frequency seen in any of the archival data we cannot claim an identification of m. If it is m = 0, then the period is 104 seconds shorter than for the m = 0 component of the 703  $\mu$ Hz group. This is not commensurate with the other two period intervals. If this mode is actually m = -1, then the m = 0 component would have a period 94.9 s longer than the 703 µHz group—which is also not commensurate. However, if the m = 0 component is 5 µHz higher in frequency (i.e., at a frequency of 763.5 µHz), then the m = 0 period for this mode is 110 s shorter than for the 703 µHz group. This number is compatible with a period spacing of 22 s.

Since an integer number of spacings must separate the periods of the modes, the difference between 1776 seconds and 1312 seconds corresponds to 21 intervals of 22.1 s. The subintervals between successive m = 0 modes are 12 intervals of 21.9 s, four intervals of 22.8 s, and five intervals of 22.0 s. With a refined estimate of the period spacing interval, we can continue this analysis and attempt to identify values of m and the number of intervals between successive modes ( $\Delta n$ ) for each of the frequencies seen in the 1991 data set (and several from the archival runs as well). Finally, a least-squares fit of the periods and  $\Delta n$ 's allows identification of the period spacing. This spacing is 22.30 seconds. Table 7 presents this model for the pulsation spectrum of NGC 1501. In all cases, the model matches the observed periods to within 4 s. Variations this large (and larger) are present in the pulsating PG 1159 stars that have been studied by WET, so the model appears to be satisfactory.

Using equation (5) of KB, and noting that this equation contains a sign error on the exponent of the luminosity term, we can use the 22.30 s period spacing to estimate the mass of NGC 1501 as  $0.55 \pm 0.03 M_{\odot}$ . The quoted uncertainty reflects the fact that the luminosity of NGC 1501 is uncertain; while Stanghellini et al. (1994) estimate an uncertainty of only about 35%, we allow that the luminosity could be anywhere between  $\approx 5000 L_{\odot}$  and  $\approx 100 L_{\odot}$  to retain a conservative error estimate in our mass determination. In addition, KB derived the relationship between mass and period spacing for PG 1159 stars, which are more highly evolved than NGC 1501; the period spacing does tend towards an asymptotic value at high luminosities in their Figure 2, however.

# 5. Summary and Conclusions

With a coordinated global observing campaign, we have obtained a high-resolution power spectrum of the pulsations of the central star of the planetary nebula NGC 1501. The star showed 10 clear periodicities during this observing run, with periods ranging from 5200 s down to 1154 s. The largest-amplitude pulsations occur between 1154 s and 2000 s. Additional data from prior years reveal that NGC 1501 changes its pulsation properties dramatically over month to year time scales. Past observations have found it pulsating with amplitudes twice as large as seen in 1991. The pulsations present in prior years in some cases occur at the same frequencies as in 1991, but in other cases the pulsations appear at different (but not random) frequencies. We note that as a PNN, NGC 1501 must be evolving relatively rapidly; with many modes seen at the same frequencies in subsequent years, we are optimistic that further analysis of the data may yield a measurement of the evolutionary change in one or more of the stable modes.

Most of the pulsation frequencies are accounted for by a simple model which includes just two input parameters. We attribute the 9.9  $\mu$ Hz spacing exhibited by several multiplets to rotational splitting, implying that the star's rotation period is 1.17 days. Moreover, there is a nearly uniform underlying period spacing of 22.30 s between the various multiplets, implying an asteroseismological mass for NGC 1501 of  $0.55 \pm 0.03 M_{\odot}$ . This mass is in close agreement with the mass determined from its position in the H–R diagram and comparison with evolutionary models (i.e., Stanghellini et al. 1994). Despite its unusual spectrum, then, NGC 1501 is a garden-variety PNN in terms of its mass; the mass we find is similar to other estimates of PNN masses. It also is consistent with the star being a progenitor of the PG 1159 spectroscopic and pulsation class.

Our success in analyzing NGC 1501 is muted by the significant observational difficulties presented by this star. NGC 1501 changes its pulsation behavior on time scales that prevent detailed monitoring. A global campaign is required to ensure that the 10  $\mu$ Hz rotational splitting is resolved from diurnal aliases, but maintaining such a vigil over the months necessary to look for changes in pulsation frequencies and amplitudes would be an enormous task. Moreover, in addition to the alias problem, there is an unfortunate degeneracy in the pulsation spectrum of this star. A period spacing of 22.30 seconds corresponds to a frequency difference of 10  $\mu$ Hz, when the periods are near 1500 s (i.e., at frequencies near 666  $\mu$ Hz). Thus the rotationally split low-frequency components of the power spectrum overlap with the consecutive overtone spacing for periods of 1500 s and longer. This may in part account for the difficulty faced in resolving this star, but unlike diurnal aliasing (which also introduces similar frequency splitting), observing from around the world does not help.

NGC 1501 is but one of nine PNNs that are now known to show nonradial g-mode pulsations (Ciardullo & Bond 1996). Data have already been obtained for RX J2117.1+3412 by the WET collaboration, and are currently being analyzed. We also have data on Sanduleak 3 that are currently being examined. With this paper's demonstration that NGC 1501 is understandable in terms of well-known principles of asteroseismology, it is our hope that the similarities between it and the other members of the class will accelerate analysis and interpretation of their pulsations. The seismological study of this fleeting stage of

stellar evolution has now begun.

HEB thanks Kitt Peak National Observatory for outstanding equipment and support, and thanks the participants for their patience during the analysis of our data. Drs. R. Kudritzki and M. Takeuti were instrumental in setting up collaborations with German and Japanese observers, respectively. SDK acknowledges the National Science Foundation for support under the NSF Young Investigator Program (Grant AST-9257049) and Grant AST-9115213 to Iowa State University. RC also acknowledges an NSF Young Investigator Grant. EML acknowledges the Israeli Academy of Sciences for supporting astronomical observations at the Wise Observatory.

#### REFERENCES

- Appleton, P. N., Kawaler, S. D., & Eitter, J. J. 1993, AJ, 106, 1973
- Bond, H.E. & Ciardullo, R.B. 1993, in White Dwarfs: Advances in Observations and Theory, edited by M.A. Barstow (Dordrecht, Kluwer), p. 491
- Bond, H.E., Ciardullo, R., & Kawaler, S.D. 1993, Acta Astr., 43, 425
- Bond, H.E., Ciardullo, R., & Meakes, M. G. 1991, in Objective-Prism and Other Surveys, in Memory of Nicholas Sanduleak, edited by A.G.D. Philip & A.R. Upgren (Schenectady, L. Davis Press), p. 91
- Bond, H.E., & Meakes, M.G. 1990, AJ, 100, 788
- Brickhill, A.J. 1975, MNRAS, 170, 404
- Buchler, J.R., Goupil, M.-J., & Serre, T. 1995, A&A, 296, 405
- Ciardullo, R., & Bond, H.E. 1996, AJ, 111, 2332
- Grauer, A.D., & Bond, H.E. 1984, ApJ, 277, 211
- Grauer, A.D., Bond, H.E., Green, R.F., & Liebert, J. 1987, in IAU Colloq. 95, The Second Conference on Faint Blue Stars, edited by A.G.D. Philip, D.S. Hayes, & J. Liebert (Schenectady, L. Davis Press), p. 231
- Heap, S. R. 1982, in IAU Symp. No. 99, Wolf-Rayet Stars: Observations, Physics, Evolution, edited by C.W.H. de Loore & A.J. Willis (Dordrecht, Reidel), p. 423
- Kaler, J.B., & Shaw, R.A. 1984, ApJ, 278, 195
- Kawaler, S.D. & Bradley, P.A. 1994, ApJ, 427, 415 (KB)
- Kawaler, S.D. et al. 1995, ApJ, 450, 350
- Nather, R.E., Winget, D.E., Clemens, J.C., Hansen, C.J., & Hine, B.P. 1990, ApJ, 361, 309
- O'Brien, M.S., Clemens, J.C., Kawaler, S.D., & Dehner, B.T. 1996, ApJ, in press
- O'Brien, M.S., et al. 1997, in preparation

- Smith, L. F., & Aller, L. H. 1969, ApJ, 157, 1245
- Stanghellini, L., Kaler, J.B., & Shaw, R.A. 1994, A&A, 291, 604
- Stetson, P.B. 1987, PASP, 99, 191
- Werner, K. 1995, Baltic Astr., 4, 340
- Werner, K., Heber, U., & Hunger K. 1991, A&A, 244, 437
- Winget, D.E., et al. 1991, ApJ, 378, 326 (WWET)
- Winget, D.E., et al. 1994, ApJ, 430, 839

This manuscript was prepared with the AAS  ${\rm IAT}_{\rm E}\!{\rm X}$  macros v4.0.

Table 1. NGC 1501 Observing Sites

Telescope	Detector	Pixel Size	Read Noise (electrons)	Filter	Exposure (s)
Kitt Peak 0.9-m	Tektronix $512 \times 512$	0".77	8	Strömgren $y$	90
Lick 1-m	GEC $288\times 385$	$0''_{.}80$	9	7500 Å	120
Okayama 0.9-m	Hamamatsu $1024\times 1024$	$0^{\prime\prime}_{\cdot}20$	15	Johnson $V$	120
Wise 1-m	RCA $320\times512$	0''.87	54	Johnson ${\cal V}$	120
Wendelstein 0.8-m	Thomson $384 \times 576$	0".47	20	Bessell $R$	120

Note. — Observers were as follows:

Kitt Peak: Bond

Lick: Stover

Okayama: Tamura, Malasan, Yamasaki, Hashimoto, Kambe, Takeuti

Wise: Leibowitz

Wendelstein: Soffner, Roth, Mitsch

Telescope	Run Name	Date (UT)	Start Time (UT)	Run Length (hh:mm:ss)
Okayama 0.9m	ok91-001	14 Nov 1991	10:11:15	9:12:56
Okayama 0.9m	ok91-002	15 Nov 1991	12:30:52	7:14:52
Okayama 0.9m	ok91-003	18 Nov 1991	13:56:26	5:51:11
Wise 1.0m	wi91-001	18 Nov 1991	16:14:16	10:52:39
Lick 1.0m	li91-001	19 Nov 1991	6:07:29	5:29:52
KPNO 0.9m	kp91-001	19 Nov 1991	7:03:58	5:54:13
Wise 1.0m	wi91-002	19 Nov 1991	16:12:40	8:24:15
Lick 1.0m	li91-002	20 Nov 1991	3:04:15	10:24:00
KPNO 0.9m	kp91-002	20 Nov 1991	3:25:54	9:15:59
Okayama 0.9m	ok91-004	20 Nov 1991	10:51:50	8:42:42
Wise 1.0m	wi91-003	20 Nov 1991	16:09:46	10:28:57
KPNO 0.9m	kp91-003	21 Nov 1991	3:17:32	9:19:01
Okayama 0.9m	ok91-005	21 Nov 1991	9:58:58	9:27:31
Wise 1.0m	wi91-004	21 Nov 1991	21:12:24	4:09:43
KPNO 0.9m	kp91-004	22 Nov 1991	2:42:46	9:51:37
Lick 1.0m	li91-003	22 Nov 1991	8:00:35	5:36:00
Okayama 0.9m	ok91-006	22 Nov 1991	9:43:32	0:48:13
Lick 1.0m	li91-004	23 Nov 1991	2:40:20	10:50:00
KPNO 0.9m	kp91-005	23 Nov 1991	3:06:07	9:33:27
Okayama 0.9m	ok91-007	23 Nov 1991	18:09:26	1:03:13
Wendelst. 0.8m	we91-001	23 Nov 1991	19:12:50	10:27:40
Lick 1.0m	li91-005	24 Nov 1991	2:36:25	7:24:51
KPNO 0.9m	kp91-006	24 Nov 1991	2:39:44	10:00:14
Okayama 0.9m	ok91-008	24 Nov 1991	9:23:14	10:38:06
Wendelst. 0.8m	we91-002	24 Nov 1991	18:24:59	8:50:19
Lick 1.0m	li91-006	25 Nov 1991	2:32:52	10:49:08
KPNO 0.9m	kp91-007	25 Nov 1991	3:08:32	9:33:40
Wendelst. 0.8m	we91-003	25 Nov 1991	16:16:09	12:54:58

Table 2. Table of observations of NGC 1501 for the 1991 global campaign

Telescope	Run Name	Date (UT)	Start Time (UT)	Run Length (hh:mm:ss)
Lick 1.0m	li91-007	26 Nov 1991	2:28:25	10:50:00
KPNO $0.9m$	kp91-008	26 Nov 1991	2:43:14	9:57:37
Wendelst. $0.8m$	we91-004	26 Nov 1991	17:01:32	12:29:07
KPNO 0.9m	kp91-009	27 Nov 1991	2:34:00	10:10:08

Table 2—Continued

Table 3. NGC1501 and its Comparison Stars

Star	$\alpha$ (J2000)	$\delta$ (J2000)	V	B-V
NGC 1501	$4^{h}06^{m}59\overset{s}{.}44$	$+60^{\circ}55'14''_{\cdot}6$	14.20	+0.71
Comp 1	$4 \ 06 \ 42.54$	$+60\ 57\ 13.6$	13.05	+0.95
$\operatorname{Comp}2$	$4\ 07\ 06.19$	$+60\ 57\ 18.4$	13.81	+0.89
Comp 3	$4 \ 06 \ 57.94$	+60 56 46.2	15.45	+1.57

Frequency	Period	Amplitude	$T_{\max}{}^{\mathrm{a}}$	comments
$(\mu { m Hz}$ )	(s)	(mma)	(s)	
$866.281 \pm 0.048$	$1154.36 \pm 0.06$	$5.00 \pm 0.37$	$132 \pm 42$	
$855.508 \pm 0.130$	$1168.90\ {\pm}0.18$	$1.84 \pm 0.37$	$1034\ \pm 115$	possible alias
$798.777\ {\pm}0.084$	$1251.91\ {\pm}0.13$	$2.66 \pm 0.36$	$872\ \pm 81$	
$758.463\ {\pm}0.044$	$1318.46\ {\pm}0.07$	$5.05 \pm 0.36$	$693~{\pm}45$	
$728.366\ {\pm}0.119$	$1372.94\ {\pm}0.22$	$1.87 \pm 0.35$	$323\ {\pm}126$	
$698.555 \pm 0.124$	$1431.53 \pm 0.25$	$1.80 \pm 0.36$	$550\ \pm 137$	
$661.089 \pm 0.121$	$1512.66 \pm 0.28$	$1.77 \pm 0.36$	$967 \pm 146$	
$567.947 \pm 0.071$	$1760.73 \pm 0.22$	$3.15 \pm 0.36$	$102 \pm 96$	
$528.275 \pm 0.088$	$1892.95 \pm 0.32$	$2.55 \pm 0.36$	$1778 \pm 128$	
$500.209 \pm 0.116$	$1999.16 \pm 0.46$	$1.92 \pm 0.36$	$198\ \pm 178$	
$191.029\ {\pm}0.059$	$5234.81 \ {\pm}1.62$	$3.73 \pm 0.36$	$4896\ {\pm}238$	

Table 4. Periodicities of NGC 1501 from 1991 Global Campaign Data.

<br/> "Time of first maximum after BJDD 2448571.50367 = 0<br/>h UT 1991 Nov14

Run name	Start Date (UT)	Start Time (UT)	Duration [h:mm:ss]
kp87-01	29 Dec 1987	4:23:46	2:25:13
kp87-02	30 Dec 1987	4:23:22	4:49:00
kp88-01	2 Jan 1988	7:00:34	3:12:10
kp88-02	27 Nov 1988	3:28:17	9:36:59
kp88-03	28 Nov 1988	1:26:43	11:39:40
kp88-04	29 Nov 1988	1:21:24	11:32:23
kp89-01	8 Oct 1989	5:50:55	6:23:22
kp89-02	9 Oct 1989	6:04:07	6:19:30
kp89-03	15 Oct 1989	4:59:51	6:40:32
kp89-04	16 Oct 1989	7:01:36	5:39:53
kp89-05	21 Oct 1989	8:42:10	2:24:34
kp90-01	1 Jan 1990	1:46:18	9:15:00
kp90-02	2 Jan 1990	1:17:52	10:01:47
kp90-03	29 Nov 1990	2:18:41	11:07:24
kp90-04	30 Nov 1990	1:42:05	11:36:33
kp90-04	3 Dec 1990	6:24:54	6:13:56
kp90-05	6 Dec 1990	7:01:34	5:40:38
кр90-00 kp90-07	0 Dec 1990 7 Dec 1990	6:52:37	5:51:30

Table 5. Archival Photometry of NGC 1501

\_\_\_\_\_

Runs	Frequency	Amplitude
	$(\mu Hz)$	(mma)
	$:569.14 \pm 0.22$	$7.7 \pm 1.6$
kp87-01,02,kp88-01	$:667.97 \pm 0.21$	$9.6 \pm 1.6$
. , , .	$795.30 \pm 0.19$	$9.4 \pm 1.6$
	$533.49 \pm 0.37$	$5.5 {\pm} 0.9$
	$558.03 \pm 0.40$	$5.2{\pm}0.9$
	$656.04 \pm 0.18$	$11.6 {\pm} 0.9$
kp88-02-04	$707.94 \pm 0.34$	$6.2{\pm}0.9$
	$729.46 \pm 0.30$	$6.9 {\pm} 0.9$
	$864.70 \pm 0.68$	$3.0{\pm}0.9$
	$900.24 \pm 0.73$	$2.8{\pm}0.9$
	$:524.92 \pm 1.20$	$5.0{\pm}1.6$
	$557.96 \pm 0.55$	$10.7 {\pm} 1.6$
	$657.39 \pm 0.61$	$9.5{\pm}1.6$
kp89-01,02	$708.08 \pm 1.40$	$5.3{\pm}1.6$
	$730.40 \pm 1.30$	$5.9{\pm}1.6$
	$:768.51 \pm 1.90$	$3.1{\pm}1.6$
	$833.19 \pm 1.00$	$5.8 {\pm} 1.6$
	$865.15 \pm 1.00$	$5.8 {\pm} 1.6$
	$532.46 \pm 0.72$	$8.5 {\pm} 1.8$
kp89-03,04	$568.12 \ {\pm}0.68$	$9.0{\pm}1.8$
	$666.25 \pm 0.48$	$12.2 \pm 1.7$
	$532.50 \pm 0.09$	$6.2 \pm 1.1$
	$558.30 \pm 0.06$	$8.7 \pm 1.1$
kp89-01-05	$655.78\ {\pm}0.05$	$9.9 \pm 1.1$
	:708.29 $\pm 0.11$	$5.0 \pm 1.2$

Table 6. Dominant Periodicities of NGC 1501 observed in archival runs.

Fig. 1.— Sample full-frame image of NGC 1501 and three comparison stars, obtained through a Strömgren y filter with the KPNO 0.9-m telescope. North is at the top, east is on the left, and the image is approximately 4.3 wide.

Fig. 2.— Combined light curve of NGC 1501 for seven days during the middle of the 1991 global campaign. Each horizontal panel represents 24 hours of data, with the UT date indicated to the right of the panel. Data from KPNO, Okayama, Wise, and Wendelstein are included in this plot; since the data from Lick overlap the KPNO data almost exactly, those data points were not plotted to retain clarity. Data from about 3 to 13 hours UT are from KPNO; from 10 to 20 hours are from Okayama; from 17 to 2 hours are from Wise; and from 20 to 5 hours are from Wendelstein.

Fig. 3.— The spectral window of the global campaign, computed by sampling a noise–free single–frequency sinusoid at the same times as present in the data. The top panel shows the power spectrum of the window function, while the bottom panel shows the amplitude spectrum.

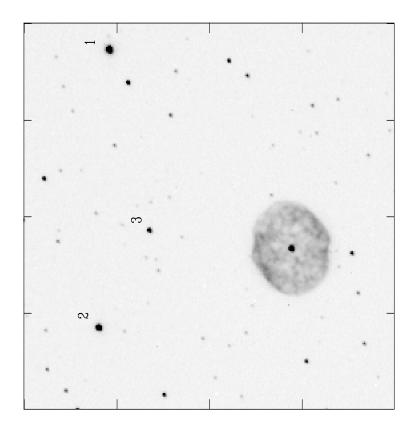
Fig. 4.— The power spectrum and amplitude spectrum of the combined data from the global campaign. The top panels show the power spectrum (and the window function) while the bottom panels show the amplitude spectrum (and the corresponding window function).

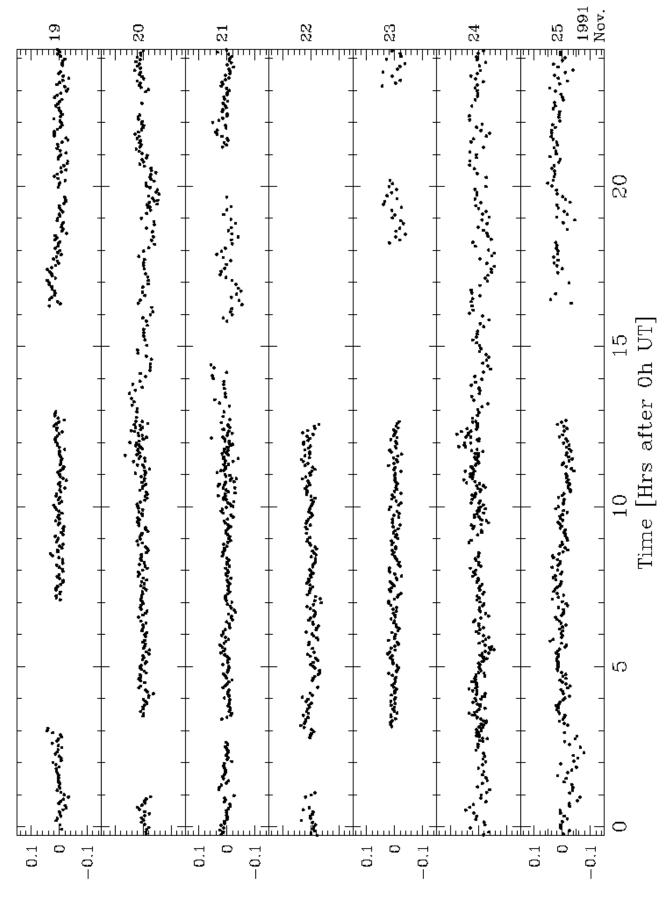
Fig. 5.— The power and amplitude spectra for the central star of NGC 1501, as observed at Kitt Peak on three consecutive nights in 1988 November. The spectra and windows are as in Figure 4. Note that the dominant peak lies at 656  $\mu$ Hz.

Fig. 6.— Enlargement of the power spectrum of the 1988 data from Kitt Peak. The solid line in each panel is the data, and the thin lines correspond to synthetic power spectra with the indicated input frequencies. See text for details of the synthesis technique. The second panel shows a good match to the observations. The bottom panel represents the window function for these runs.

Runs	Frequency	Amplitude
	$(\mu { m Hz}$ )	(mma)
		50 110
	$:730.31 \pm 0.11$	
	$:768.93 \pm 0.12$	$4.4 \pm 1.1$
	$865.89\ {\pm}0.09$	$5.1~{\pm}1.1$
	:533.84 $\pm 0.78$	$5.3\ \pm 1.1$
	:557.64 $\pm 0.76$	$5.5 \pm 1.1$
kp90-01,02	$655.78\ {\pm}0.45$	$9.1~{\pm}1.1$
	$707.85\ {\pm}0.79$	$5.2\ \pm 1.2$
	$728.97\ {\pm}0.89$	$4.7 \pm 1.2$
	$865.87\ {\pm}0.62$	$6.5 \pm 1.1$
	$655.75\ {\pm}0.91$	$5.1 \pm 1.3$
kp90-03,04	$695.86 \ {\pm}0.47$	$9.8 \pm 1.3$
	$758.52\ {\pm}0.61$	$7.4 \pm 1.5$
	$864.33\ {\pm}0.76$	$5.9 \pm 1.3$

Table 6—Continued





Modulation Intensity

